Reprinted from JOURNAL OF ENERGY, Vol. 2, No. 5, September–October, 1978, pp. 269–278

Modeling and Simulation of a Multicell Fluidized-Bed Steam Generator

Asok Ray,* David A. Berkowitz,† and Venilal H. Sumaria*
The MITRE Corporation, Bedford, Mass.

A nonlinear dynamic model of a multicell, atmospheric-pressure, fluidized-bed combustion steam generator is developed in state-space form. All model parameters are physical quantities derived from design data, and the model can be readily adapted to other fluidized-bed combustion steam generators. Steady-state performance of the nonlinear model is predicted at 100, 87.5, and 75% load levels, and local stability is examined in this range. Frequency response characteristics of several system variables and transient response of the system following a coal feed rate disturbance are presented to illustrate use of the model.

Nomenclature

A	= area
C	= specific heat
F	= fluid flow rate
H	= fuel heating value, effective
h	= specific enthalpy
K	= constant
k	= thermal conductivity of tube material
l	= length
M	= flow rate of solid materials
m	= mass
p	= fluid pressure
Q	= heat-transfer rate
r	= tube radius
T	= temperature
t	= time
u	= specific internal energy
v	= volume
α	= part of Q_b^* due to conduction and convection
β	= part of M_f consumed in bed
η	= exponent for convective heat-transfer coefficient
Θ	= conversion factor to absolute temperature
ρ	= density
τ	= time constant related to fuel residence time

Superscripts

$( )^*$	= design condition

Subscripts

a	= average
at	= attemperator
b;bg;bz	= bed; gaseous products in bed; solid materials in bed
bl	= boiling
c	= cell
d	= air damper
e	= elutriated material
eo	= economizer outlet
f;fx	= fuel; fraction consumed in bed
fd	= forced draft fan
fg	= flue gas
fi;fo	= air inlet plenum; flue gas exhaust duct (air preheater gas inlet)
fw	= feedwater
i	= inlet, inner
id	= induced draft fan
l	= limestone
m;mi;mo	= tube material; inner surface; outer surface
o	= outlet, outer
pa;pg	= air at constant pressure; gas at constant pressure
q	= carrier air
s;ss	= saturated steam; superheated steam
sv	= steam valve
t	= fluidized air
u	= dumped materials from bed
vg	= gas at constant volume
w	= saturated water

Received Jan. 27, 1978; revision received May 22, 1978.

Index categories: Powerplant Design; Simulation.

*Technical Staff Member.
†Group Leader.

Introduction

WITH increasing demand for electric power, rising fuel oil prices, and continual re-evaluation of nuclear power, use of coal for commercial power generation has regained importance. Environmental requirements prevent the use of high-sulfur coal in conventional pulverized fuel (PF) power plants; however, fluidized-bed combustion provides an attractive alternative for efficient SO_2 removal.

Several fluidized-bed combustion (FBC) facilities with equivalent capacities in the range 1-10 MW_e are operational at present, or in various stages of design and construction.[1] A 30-MW_e multicell unit installed at Monongahela Power Company's Rivesville Station in West Virginia is now being tested. 200 MW_e plants suitable for commercial use by utility companies are being considered. This technology is being developed much more rapidly than has been the case with conventional fossil power plants. Mathematical modeling and simulation are useful tools for analyzing performance and control problems in complex, interactive systems such as power plants;[2,3] their application to FBC systems is very timely.

This paper describes a nonlinear dynamic model of the 6-MW_e multicell atmospheric-pressure FBC Component Test and Integration Unit (CTIU) to be built at Morgantown Energy Research Center, West Virginia.[4,5] The model is suitable for digital simulation and analytical controller design, and provides the basis for: 1) understanding interactive process dynamics, 2) design verification and predicting effects of subsystem changes on the entire process, 3) interactive multivariable controller design, and 4) overall system (process and controller) performance evaluation. The modeling method has been experimentally verified in a single-

cell FBC test plant.[1,6] The modeling and simulation techniques presented in this paper have general applicability and can be readily adapted to study other FBC steam power generation systems.

System Description

In fluidized-bed combustion, coal particles of about 1-cm top size are introduced pneumatically into a coarse bed of calcined limestone (average bed particle dimension is about 3 mm). At any instant, the bed coal fraction is about 2%, and once coal has ignited, combustion is self-sustaining. Coal separates into a volatile component and a solid component of char and ash. A portion of the char and ash is blown out of the bed or elutriated.

Calcined limestone, CaO, acts as the SO_2 sorbent. It reacts with O_2 and SO_2 in the bed to form $CaSO_4$. As the amount of available limestone decreases, fresh limestone is added which calcines in the bed. With continual addition of fresh bed material, spent bed material must be removed to maintain constant bed mass or bed height. In addition, continuous bed recirculation and screening remove bed materials that do not react.

To optimize sorbent effectiveness and to avoid ash sticking and agglomerating, fludized-bed temperature is controlled at approximately 840° C (1550° F). Thermal energy is continually removed from the bed by water- or steam-cooled heat-transfer surface. Use of immersed heat-transfer assemblies gives the fluidized-bed boiler its major distinctive feature, creating at the same time several advantages and several new problems.[7]

Three fluidized-bed cells, arranged vertically, comprise the CTIU atmospheric-pressure fluidized-bed steam generator. Figure 1 is the simplified plant schematic suitable for normal operating conditions which is used for modeling.

Fluidizing air from the forced draft (FD) fan is preheated by flue gas in a shell-and-tube heat exchanger. Flue gas from cells A and B is combined and passed through a cyclone to remove ash and unburnt coal (which is recycled into cell C, the carbon burn-up cell) and then, together with flue gas from cell C, is cooled in the air preheater.[4] Flue gas leaving the air preheater is further cleaned in the bag filter collector, then discharged to the stack via the induced draft (ID) fan.

The steam supply system incorporates economizer, steam drum, and superheaters. Feedwater passes through feedwater heaters and an economizer in the cell C convection zone into the drum. Saturated drum water passes by forced circulation through waterwalls of all three cells, and cell A and cell B evaporators. Waterwalls cover the entire length of each cell and are exposed to fluidized-bed, freeboard, and convection zones. Effective heat-transfer area can be modified by addition of refractory insulation covering part of the waterwalls. Evaporators are located in the convection zones of cells A and B, and in the bed of cell B. Saturated drum steam is superheated in tubes immersed in the bed of cell A; final steam temperature is regulated by feedwater spray introduced between two stages of the superheater. Steam flow is regulated by a control valve analogous to governor valves in a steam turbine-generator.

Modeling Approach

The purpose of modeling is to describe overall system performance and component interaction with sufficient accuracy for controller design, rather than to describe microscopic process details occurring within individual components, which relates more to component design. If the system model incorporated detailed component models, computer runs would be too costly, particularly for long simulations. The present approach emphasizes component interaction.

The physical process consists of distributed parameter dynamic elements, mathematically represented by nonlinear partial differential equations with space and time as independent variables. A lumped parameter approximation is used to formulate a finite-dimensional state space model. Partial differential equations are reduced to a set of ordinary differential equations with time as the independent variable. This approach has been shown to be adequate in the simulation of other power plants.[8-10]

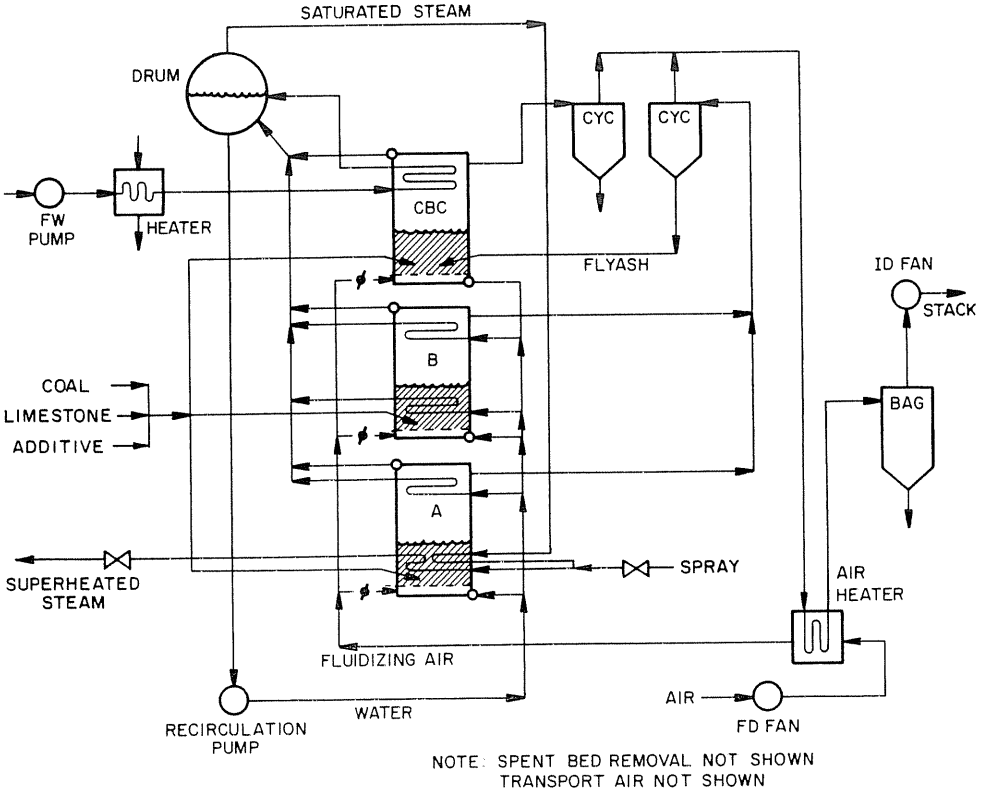

Fig. 1 Simplified plant schematic.

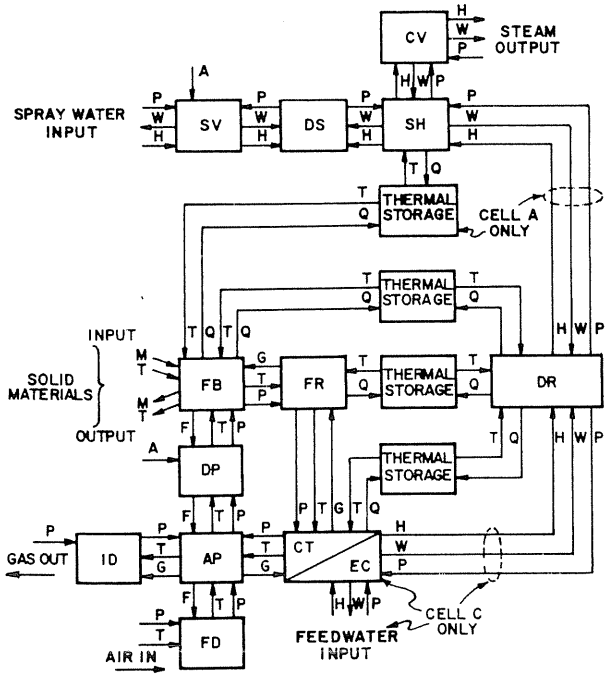

NOMENCLATURE

A NORMALIZED VALVE OR DAMPER AREA	AP AIR PREHEATER
F MASS FLOWRATE OF AIR	CT CONVECTION TUBES (CELLS A, B EVAPORATORS)
G MASS FLOWRATE OF FLUE GAS	CV STEAM CONTROL VALVE
H SPECIFIC ENTHALPY, WATER OR STEAM	DP DAMPERS (CELLS A,B,C)
M MASS FLOWRATE, SOLID MATERIALS	DR DRUM LOOP AND WATER WALLS
P PRESSURE	DS DESUPERHEATER
Q HEAT TRANSFER RATE	EC ECONOMIZER (CELL C ONLY)
T TEMPERATURE	FB FLUIDIZED BED (CELLS A,B,C)
W MASS FLOWRATE, WATER OR STEAM	FD FORCED DRAFT FAN
	FR FREEBOARD (CELLS A,B,C)
	ID INDUCED DRAFT FAN
	SH SUPERHEATER (CELL A ONLY)
	SV SPRAY WATER CONTROL VALVE

NOTE: WATER/STEAM FLOW FOLLOWS THE DIRECTION OF H. AIR/GAS FLOW FOLLOWS THE DIRECTION OF T.

Fig. 2 Model solution diagram

A model solution diagram for the fluidized-bed plant is shown in Fig. 2. Each block in the diagram represents a group of physical components. Lines interconnecting blocks indicate direction of information flow or "model causality." This diagram shows how individual component models mathematically interface with each other, and insures consistent causality for the complete set of equations defining the physical process.

Following the arrangement in Fig. 2, plant modeling is accomplished in two steps: 1) modeling of individual components or groups of components and 2) formulation of an overall plant model by appropriate interconnection of individual component models. Step 1 includes determination of steady-state solutions and eigenvalues (of linearized models) at several operating points. Steady-state solutions are verified with design data, and eigenvalues are examined for frequency range. Step 2 incorporates sequential interconnection of component models according to the solution diagram. Steady-state solutions and eigenvalues of the augmented models are examined at each phase of interconnection.

Model equations are formulated from: conservation relations for mass, momentum, and energy; semiempirical relationships for fluid flow and heat transfer; and state relations for thermodynamic properties of working fluids. Major assumptions in addition to the lumped parameter approximation are: 1) uniform fluid flow over pipe, duct, or furnace cross section; 2) perfect thermal insulation between plant components and the environment; 3) negligible pressure

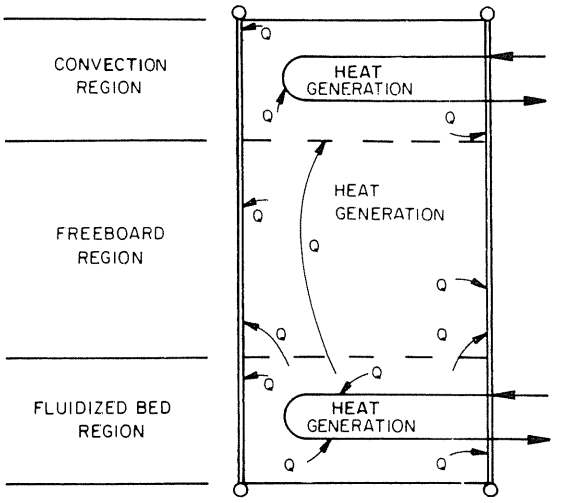

CONVECTION REGION: HEAT TRANSFER TO WATERWALLS BY CONVECTION, AND TO PENDANT TUBES BY CONVECTION AND RADIATION

FREEBOARD REGION: HEAT TRANSFER TO WATERWALLS BY CONVECTION AND RADIATION

FLUIDIZED BED REGION: HEAT TRANSFER BY CONDUCTION, CONVECTION, AND RADIATION

Fig. 3 Heat-transfer regions of fluidized-bed cell.

drop due to velocity and gravitational heads in gas and steam paths; 4) uniform fluidized-bed temperature; 5) coal division into solid and gas fractions independent of sulfur concentration; 6) in-bed heat-transfer coefficient independent of superficial air velocity; 7) constant average value of coal particle residence time in the fluidized bed; 8) elutriation rate proportional to total air flow; and 9) overbed combustion rate proportional to air flow and in-bed combustion rate. Assumptions 1, 2, and 3 have been used in modeling conventional steam generators.[8-11] Assumptions 4 through 9, which will be discussed more fully in the following section, are unique to the fluidized-bed system and reflect areas of current research, such as heat-transfer coefficients, flue gas residence time, bed depth, etc. In the model reported here, simple relations or constant input values have been assumed for certain variables and parameters. The model structure permits them to be readily changed or replaced when more appropriate information is available.

In utilizing the model, it is assumed that for the particular coal and limestone being utilized, and for their respective bed particle size distributions, coal residence time and elutriation rate, for example, will be calculated initially and used as model input parameters. The purpose of the model is not to determine such parameters which pertain primarily to processes occuring within the bed itself, but rather to study their effect on the overall steam generator.

Development of Model Equations

The plant model has 36 first-order nonlinear differential equations, plus many supporting algebraic relationships. Detailed derivations are too extensive for presentation here, but are available in Ref. 12. A list of state, control (input) and output variables is given in the Appendix. This section is a discussion of plant components and processes. Key functional relationships are included to illustrate modeling philosophy, the physical and empirical bases for constructing mathematical descriptions, and the level of approximation that has been employed.

Heat Transfer

Coal combustion takes place primarily in the fluidized bed, but some overbed combustion occurs in the freeboard and convection regions. For modeling purposes, each cell is

divided into three regions: fluidized bed, freeboard, and convection pass as shown in Fig. 3.

Experimental data from the Alexandria fluidized-bed Process Development Unit operating at different load levels show that heat transfer to immersed tubes can be split into a linear part due to conduction and convection and a nonlinear part due to radiation:[1,6]

$$Q_b = K_b l\left[\alpha + (1-\alpha)\left(\frac{T_b + T_{mo} + 2\Theta}{T_b^* + T_{mo}^* + 2\Theta}\right)\right.$$
$$\left.\times\left(\frac{(T_b+\Theta)^2 + (T_{mo}+\Theta)^2}{(T_b^*+\Theta)^2 + (T_{mo}^*+\Theta)^2}\right)\right](T_b - T_{mo}) \quad (1)$$

α is the fraction of total heat transfer due to conduction and convection at the design load condition, for which $T_b = T_b^*$ and $T_{mo} = T_{mo}^*$. Parameters K_b and α can be evaluated from steady-state experimental or design data at two different operating conditions. Since design data are available at only one operating point, the value $\alpha = 0.5$ was assumed based on earlier test results,[1,6] and K_b was calculated from design data. Equation (1) is applied separately to horizontal and vertical immersed heat-transfer surfaces.

Heat transfer from waterwall inner surface to water/steam mixture is obtained using the empirical correlation of Thom et al.[13] for nucleate boiling:

$$Q_{bl} \propto [\exp(p_s)](T_{mi} - T_s)^2 \quad (2)$$

Conductive heat transfer through tubewalls is assumed radial:

$$Q_{bl} = \frac{A_i k}{r_i \ell_n (r_o/r_i)}(T_{mo} - T_{mi}) \quad (3)$$

Equations (2) and (3), applied separately in each cell, are solved simultaneously for Q_{bl} eliminating T_{mi}.

Convective heat transfer in the freeboard convection region and air preheater are computed using well-established formulas.[13-15] Heat-transfer coefficients are assumed flow-dependent only;[8-11] dependence on variations in fluid properties is not significant, in comparison. Convective heat-transfer rate in each heat-transfer assembly has the form

$$Q \propto AF^{\eta}(\Delta T) \quad (4)$$

The proportionality constant is determined using fluid properties at mean thermodynamic conditions.

Radiative heat transfer above the bed,

$$Q \propto [(T_b+\Theta)^4 - (T_{mo}+\Theta)^4] \quad (5)$$

is applied separately to freeboard and convective regions. The proportionality constant includes emissivity, effective surface area, and the Stefan-Boltzman constant.[15]

Freeboard and Convection Regions

In the absence of a validated, analytical relation in terms of air flow rate, type and size distribution of coal and bed material, etc., overbed combustion rate is assumed proportional to elutriation rate and to coal combustion rate in the bed. The proportionality constant is calculated from steady-state design data for the particular coal type and bed material being employed.

In the freeboard (see Fig. 3), average gas temperature is selected as a state variable for the lumped thermal capacitance associated with flue gas and elutriated solids. Its governing equation is derived from dynamic energy balance, neglecting flue gas compressibility to avoid numerical integration.

Flue gas temperatures entering and leaving the convection region are obtained assuming fixed averaging constants which can be chosen for linear or log-mean temperature differences.

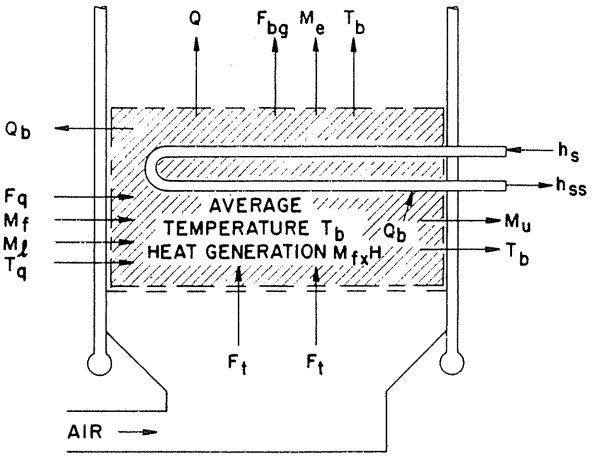

Fig. 4 Fluidized-bed control volume.

Convection region gas volume is small; average gas temperature is computed algebraically to avoid numerical instability due to fast transients.

Fluidized Bed

The control volume selected for modeling fluidized-bed dynamics is shown in Fig. 4. Its top surface determines bed depth, which is a function of time-dependent process variables such as superficial velocity, mass of solid bed materials, etc. A fixed fluidized-bed control volume is assumed as a first approximation on the basis of existing experimental data.[1,6] Heat-transfer areas are automatically adjusted for the input value of bed depth. A time-varying control volume[11] can be incorporated into the model with little difficulty when a suitable analytical relationship for bed depth becomes available.

Mass conservation in the control volume yields

$$\frac{d}{dt}(m_{bg} + m_{bz}) = M_f + M_l + F_t + F_q - F_{b_g} - M_e - M_u \quad (6)$$

Air and flue gas dynamics inside the cell are very fast, with time constants less than a few milliseconds. Control systems and measuring instruments are low-pass filters with respect to such transients, which will have little bearing on overall process dynamics and controller design. Thus dm_{bg}/dt is set to zero, and flue gas flow leaving the cell is computed algebraically by direct mass balance with air flow and instantaneous rate of coal combustion M_{fx}. This is equivalent to setting one eigenvalue of the linearized system to negative infinity. Dynamics of mass storage in the bed reduce to

$$\frac{d}{dt}(m_{bz}) = M_f + M_l - M_{fx} - M_e - M_u \quad (7)$$

Bed mass in the fluidized-bed furnace is analogous to water level in a drum boiler; it behaves as a free integrator in the absence of level control. Rather than postulate a feedback controller whose characteristics could influence mass storage dynamics, an ideal controller is assumed which brings bed mass to steady-state value instantaneously, and

$$\frac{d}{dt}(m_{bz}) = 0 \qquad M_u = M_f + M_l - M_{fx} - M_e \quad (8)$$

This separates process dynamics from control dynamics, which can be added subsequently when the controller is developed for all aspects of the process: combustion, steam generation, flow gas composition, as well as drum level and bed level.

The coal sulfur fraction adds to bed mass by the sulfation reaction. CO_2 evolution by calcination of freshly added limestone reduces bed mass. For a Ca:S mol ratio of 2, the gain and loss in bed mass approximately balance and these effects are ignored in the model.

Mass flow of elutriated solids varies with total air flow, to which it is assumed proportional:

$$M_u = K_u (F_t + F_q) \tag{9}$$

The proportionality constant is characteristic of the coal and bed material being used.

Coal combustion dynamics inside the bed are approximated by a first-order lag.

$$M_{fx} = \frac{m_f}{\tau} \qquad \frac{dM_{fx}}{dt} = \frac{1}{\tau}\frac{dm_f}{dt} = \frac{1}{\tau}(\beta M_f - M_{fx}) \tag{10}$$

Coal introduced into the burning bed has a volatile component which burns in a few seconds, and a solid char component which burns more slowly;[16] mass fractions for each component are often comparable. In Eq. (10), τ is related to an average residence time assumed to be a characteristic of the coal being burned, including its char reaction rate and fractional partition into volatile and solid components. Although an Arrhenius temperature dependence of char reaction rate could be included in τ, the simplifying assumption of temperature independence has been made for the following reasons: 1) rapid combustion of the volatile component diminishes the effect of char combustion rate temperature dependence; 2) in normal operation, during which stable combustion is assumed, the range of bed temperature variation will be kept small (perhaps $\pm 60°C$); and 3) in terms of overall steam generator performance, thermal relaxation time of stored energy in the bed (a very slow process) has a much greater effect on system response than changes in char combustion rate.

In this paper, $\tau = 60$ s is assumed for cells A and B, and $\tau = 10$ s for cell C, in which fuel is predominantly elutriated coal fines. A more detailed functional relationship can be incorporated in the model when available. Similarly, β, the coal fraction consumed in the bed, is assumed to be a constant characteristic of the coal type and bed material; it can also be replaced by some other functional relationship if necessary. System sensitivity to τ and β can be readily investigated with the model. Results of a similarly formulated model for the Alexandria FBC steam generator, incorporating the preceding simplifying assumptions, agreed closely with experimental data.[1,6]

Thermal energy released in the bed by combustion is obtained from an effective coal heating value (due to combined effects of combustion, calcination, and sulfation reactions) and instantaneous combustion rate. Average bed temperature (selected as a state variable) provides dynamic information about fluidized-bed energy storage. The governing equation is obtained from dynamic energy balance for gases and solids in the control volume (see Fig. 4):

$$\begin{aligned} dT_b/dt = [&(M_f C_f + M_l C_l) T_q - (M_e + M_u) C_{bz} T_b \\ &+ (F_t T_t + F_q T_q) C_{pa} - F_{bg} T_b C_{pg} + M_{f_x} H - \Sigma Q_b] \\ &\div (m_{bz} C_{bz} + m_{bg} C_{vg}) \end{aligned} \tag{11}$$

ΣQ_b is total heat-transfer rate from bed.

Air and Gas Flow

Main air flow, regulated by a damper in each cell, is computed from pressure drop across the ducts, damper, distributor plate, and fluidized bed. Flow is expressed in terms of inlet and exit pressures, and average density:[1]

$$F \propto \sqrt{(p_i - p_o)\rho_a} \tag{12}$$

Assuming constant spatial temperature distribution, average density is approximately proportional to average pressure, $p_a = (p_i + p_o)/2$, which yields a simple algebraic expression for main air flow to each cell in terms of FD fan pressure, bed pressure, and damper area:

$$F_t = K_d A_d \sqrt{(p_{fi}^2 - p_c^2)} \tag{13}$$

Portions of elutriated materials are converted to flue gas in each cell by overbed combustion. Flue gas flow F_{fg} leaving each cell is the sum of gas flow F_{b_g} and total rate of overbed combustion. F_{fg} is also obtained from cell pressure and exhaust duct pressure in a form similar to Eq. (13). Air flow through each cell is then algebraically computed in terms of air inlet plenum pressure and exhaust duct pressure. Assuming no leakage, air flow through the forced draft (FD) fan and air preheater is the sum of air flow through cells A, B, and C.

FD fan pressure is a constant input parameter. Pressure drop from FD fan to furnace inlet plenum (upstream of cell inlet dampers) is assumed proportional to air flow squared; thus, inlet plenum pressure depends on air flow. To avoid an implicit algebraic loop, air flow is assumed directly proportional to feedwater flow, which reflects the manner in which plants are normally operated. Therefore,

$$p_{fi} = p_{fd} - \Delta p^* (F_{fw}/F_{fw}^*)^2 \tag{14}$$

where Δp^* is the rated value of the FD fan to air inlet plenum pressure drop.

To avoid numerical integration difficulties due to very fast transient effects, air/flue gas flow dynamics are represented by a single lumped node at the air preheater gas inlet. Dynamic mass and energy balance yield

$$\frac{d}{dt}(\rho_{fo}) = \frac{\Sigma F_{fg} - F_{id}}{V_{fo}} \tag{15}$$

$$\frac{d}{dt}(\rho_{fo} T_{fo}) = \frac{(C_{pg}/C_{vg})[\Sigma F_{fg} T_{co} - F_{id} T_{fo}]}{V_{fo}} \tag{16}$$

where Σ indicates summation over cells A, B, and C.

Flue gas pressure p_{fo} at the air preheater gas inlet is obtained from T_{fo}, ρ_{fo}, and the perfect gas law (assuming fixed average flue gas chemical composition). Flue gas flow F_{id} through the air preheater, bag filter, and the induced draft (ID) fan is computed from the pressure difference between exhaust duct and ID fan inlet [see Eq. (13)].

Cell A and Superheater Subsystem

Dynamic energy balance in the three regions of each cell (see Fig. 3) yields governing equations for respective tube temperatures. Boiling heat transfer from tube wall to water/steam is obtained from Eqs. (2) and (3) with appropriate tube wall temperatures and heat-transfer areas. Lumped thermal capacitance in the bed and freeboard regions varies in proportion to bed depth, in one case increasing, in the other decreasing. Void fraction of steam in the waterwalls varies with firing rate; hence, lumped average thermal capacitances change with load even if bed depth remains constant. However, variations in thermal capacitance of the fluid are small in comparison to the combined average thermal capacitance of tube material and fluid, and this effect is neglected.

In primary and secondary superheaters, steady-state forms of continuity, momentum, and energy equations are used because of relatively small control volumes.

Heat transfer to steam in the primary or secondary superheater is[11]

$$Q \propto [\gamma + (1-\gamma)(F_{ss}/F_{ss}^*)^{-\eta}](T_{mo} - T_{ss}) \tag{17}$$

where γ is the portion of thermal resistance due to conductive heat transfer through the tube wall.

Average superheater steam temperatures are obtained using thermodynamic state relationships in the form

$$T_{ss} = f_1(p_{ss}) + h_{ss} f_2(p_{ss}) \tag{18}$$

Average steam pressure and enthalpy are obtained by linear interpolation between inlet and outlet conditions. Tube wall thermal dynamics are obtained separately for both primary and secondary superheaters by energy balance between the bed and steam.

Average steam density ρ_{at} and enthalpy h_{at} are chosen as state variables in the attemperator control volume, which is larger than primary and secondary superheater volumes. Governing equations are derived from dynamic mass and energy balance relations.[18]

Flow of superheated steam from cell A is regulated by the main steam valve. In normal operation, pressure ratio across this valve is always greater than 2, and the flow is choked.

$$F_{sv} \propto A_{sv} \sqrt{p_{sv} \rho_{sv}} \tag{19}$$

Additional control volume is associated with the pipe length leading to the steam flow control valve. Steam density ρ_{sv} and enthalpy h_{sv} are chosen as state variables, with governing equations derived as previously from continuity and energy conservation equations.[18]

Cell B Subsystem

Model equations for cell B are identical to those for cell A, except immersed heat-transfer tubes are for boiling, and are included in the drum recirculation loop.

Cell C Subsystem

Cell C is a carbon burn-up cell with no immersed heat-transfer surface except a portion of the waterwalls. Convection tubes above the freeboard are the economizer. Other model equations in cell C are identical to those in cell A.

Economizer tube temperature is selected as a state variable; the governing equation is obtained from dynamic energy balance in the combined tube wall and water control volume. Heat transfer from tube wall outer surface to water is by conduction and convection, and has a form similar to Eq. (17).

Steam Generator and Drum Subsystem

The drum model is formulated using established techniques assuming saturated conditions, uniform drum pressure, and constant flow through each recirculation pump.[9] Mass and energy conservation in the drum control volume yield

$$\frac{d}{dt}(\rho_s V_s + \rho_w V_w) = F_{fw} - F_{ss} \tag{20}$$

$$\frac{d}{dt}(\rho_s V_s u_s + \rho_w V_w u_w) = F_{fw} h_{eo} - F_{ss} h_s + \Sigma Q_{bl} \tag{21}$$

ΣQ_{bl} is the total heat-transfer rate to water/steam in waterwalls and evaporators of all three cells. ρ_s and V_w are selected as state variables. Thermodynamic properties of water and steam at saturated conditions are expressed as functions of ρ_s, and using partial derivatives with respect to ρ_s as well, Eqs. (20) and (21) are solved simultaneously for $d\rho_s/dt$ and dV_w/dt.

Feedwater flow F_{fw} is determined by feed pump-to-drum pressure drop across the pipe and flow control valve. Drum water volume acts as a free integrator; an ideal controller has been assumed which balances feedwater and steam flow at every instant, and maintains V_w at the desired constant value.

Gas Emission Characteristics

In a fluidized-bed steam generator, limestone feed rate is controlled on the basis of SO_2 concentration in the flue gas, while air flow and coal feed rates are influenced by O_2 concentration. In order to apply the model to limestone and excess-O_2 controller design, these concentrations must be available as output variables using equations describing fluidized-bed chemical kinetics. This is a subject of current research, and has not been included in this paper. Since dynamics of flue gas composition do not interact strongly with heat-transfer processes in the bed, freeboard, or convection regions, the model is adequate for describing dynamics of steam generation in a fluidized-bed boiler.

Model Results

The nonlinear model has been used to simulate plant performance for both steady-state operation and transient responses following selected disturbances, and has been linearized at several operating points to investigate local stability and frequency response.

Steady State

Model parameters were calculated from design data at 100% load. A controller was added to the process to steer it to other operating levels. Inputs to the (closed-loop) process and controller model are desired set-point values of steam flow (taken as the load index), steam pressure, and steam temperature, and average bed temperatures in cells A, B, and C.

Table 1 shows predicted steady-state performance of the nonlinear process model at 100, 87.5, and 75% rated steam flow. Set-point values of steam conditions and cell C bed temperature were held constant. Cell A and cell B bed temperatures were reduced at the lower loads because heat transfer to immersed surfaces is primarily dependent on bed temperature, and some method is needed to reduce it. Otherwise, load reduction at constant bed temperatures would require very large decreases in fluidizing air flow in order to decrease heat transfer in freeboard and convective regions, resulting in unacceptable air-to-fuel ratios.

For turndown to even lower loads, bed slumping or other means of heat-transfer area reduction should be explored. Although such investigations have not been made in this study, the model would be useful for that purpose.

System Eigenvalues

For a nonlinear model in state-space form, small signal stability about a steady-state operating point can be determined by linearizing the model at that operating point to determine system eigenvalues. The eigenvalues at 100, 87.5, and 75% load levels are given in Table 2. All have negative real parts, showing that the system, as modeled, is stable. Some eigenvalues vary significantly with load, illustrating the effect of nonlinear plant characteristics. The magnitude of most eigenvalues decreases monotonically at lower loads showing that process response becomes progressively slower. A controller design based solely on the plant model at high load may yield unsatisfactory performance at lower loads.

Frequency Response

Transfer functions of several output variables with respect to controlled inputs were obtained from the linearized models at different load levels. For example, frequency response of cell A and cell B bed temperatures with respect to cell A coal feed rate is given in Figs. 5 and 6, respectively.

The transfer function of cell A bed temperature with respect to cell A coal feed rate can be approximated by a simple structure of three finite poles. Since the magnitude attenuates rapidly with increasing frequency, derivative control action would result in fast closed-loop response. Transfer function analysis is useful for single-input single-output controller design, and is a first step toward an interactive multivariable approach.

Table 1 Predicted steady-state performance

Description		Percent rated steam flow 100	87.5	75
Main steam pressure	psia	500.00	500.00	500.00
	10^6 N/m^2	3.447	3.447	3.447
Main steam flow	10^3 lb$_m$/h	63.000	55.125	47.250
	kg/s	7.937	6.944	5.952
Main steam temperature	°F	625.00	625.00	625.00
	°C	329.44	329.44	329.44
Drum steam pressure	psia	560.40	547.46	535.66
	10^6 N/m^2	3.864	3.775	3.693
Stack flue gas temperature	°F	311.6	297.1	278.6
	°C	155.33	147.3	137.0
Cell A bed temperature	°F	1550.00	1450.00	1350.00
	°C	843.33	787.78	732.22
Cell A fuel flow	10^3 lb$_m$/h	2.382	2.063	1.749
	kg/s	0.300	0.260	0.220
Cell A air flow	10^3 lb$_m$/h	24.624	23.863	22.156
	kg/s	3.102	3.006	2.791
Cell B bed temperature	°F	1550.00	1450.00	1350.00
	°C	843.33	787.78	732.22
Cell B fuel flow	10^3 lb$_m$/h	2.686	2.312	1.949
	kg/s	0.338	0.291	0.235
Cell B air flow	10^3 lb$_m$/h	19.584	18.653	16.604
	kg/s	2.467	2.350	2.092
Cell C bed temperature	°F	1780.00	1780.00	1780.00
	°C	971.11	971.11	971.11
Cell C flyash & fuel flow	10^3 lb$_m$/h	1.364	1.356	1.330
	kg/s	0.172	0.171	0.168
Cell C air flow	10^3 lb$_m$/h	5.724	5.512	5.017
	kg/s	0.721	0.694	0.632

Table 2 System eigenvalues (s^{-1}) of the linearized plant model[a]

Percent rated steam flow 100	87.5	75
−0.169 E−2	−0.156 E−2	−0.140 E−2
−0.232 E−2	−0.229 E−2	−0.224 E−2
−0.328 E−2	−0.283 E−2	−0.245 E−2
−0.554 E−2	−0.528 E−2	−0.485 E−2
−0.167 E−1	−0.167 E−1	−0.167 E−1
−0.167 E−1	−0.167 E−1	−0.167 E−1
−0.225 E−1	−0.200 E−1	−0.173 E−1
−0.227 E−1	−0.205 E−1	−0.182 E−1
−0.310 E−1	−0.299 E−1	−0.274 E−1
−0.373 E−1	−0.334 E−1	−0.295 E−1
−0.807 E−1	−0.804 E−1	−0.792 E−1
−0.861 E−1	−0.834 E−1	−0.806 E−1
−0.906 E−1	−0.881 E−1	−0.849 E−1
−0.972 E−1	−0.957 E−1	−0.892 E−1
−0.987 E−1	−0.970 E−1	−0.941 E−1
−0.100	−0.100	−0.950 E−1
−0.103	−0.101	−0.977 E−1
−0.106	−0.101	−0.100
−0.108	−0.104	−0.101
−0.110	−0.107	−0.104
−0.120	−0.118	−0.113
−0.134	−0.128	−0.116
−0.147	−0.132	−0.125
−0.178	−0.174	−0.170
−0.468	−0.436	−0.382
−0.577	−0.504	−0.467
−0.122 E+1	−0.118 E+1	−0.109 E+1
−0.154 E+1	−0.145 E+1	−0.130 E+1
−0.189 E+1	−0.181 E+1	−0.168 E+1
−0.234 E+1	−0.252 E+1	−0.278 E+1
−0.351 E+1	−0.353 E+1	−0.364 E+1
−0.657 E+1	−0.724 E+1	−0.819 E+1

[a] All system eigenvalues at each flow condition are real.

Frequency response of cell B bed temperature with respect to cell A coal feed rate is shown in Fig. 6; the transfer function can be approximated by four finite poles and one finite zero. The dependence of cell B process dynamics on cell A fuel input disturbance demonstrates the interactive nature of a multicell arrangement; this point is discussed further in the next section on transient response.

The classical transfer function approach can be extended to feedback controller design for interactive multivariable systems using established design algorithms.[19] For this purpose, a family of transfer function matrices can be generated from linearized versions of the model.

Transient Response

Figures 7a, b, and c show transient response of steam pressure, temperature, and flow, cell A and cell B bed temperatures, and fluidizing air flow following independent disturbances in cell B coal feed rate, cell B air damper position, and main steam valve position, respectively. During these runs, initial cell B bed temperature was 760°C (1400°F) in anticipation of a temperature increase following the step change in coal feed rate. Disturbances were applied to the open-loop process at zero minutes following a period of steady-state operation at 100% load.

Following a +5% step change in cell B coal feed rate (Fig. 7a), cell B bed temperature increases monotonically to a higher steady-state value (1476°F). Increased firing rate also increases furnace exit pressure where hot flue gas from all three cells mix. Cell A bed temperature increases slightly (2°F) as air flow through cell A decreases (−0.34%) in response to the higher furnace exit pressure. This illustrates the interactive nature of the process. Drum steam pressure and temperature also increase because of greater heat absorption in waterwall and evaporator tubes resulting in more rapid boiling. Consequently, main steam pressure, temperature, and flow increase.

Following an 11% step decrease in cell B air damper area corresponding to an 8.3% decrease in air flow at steady state

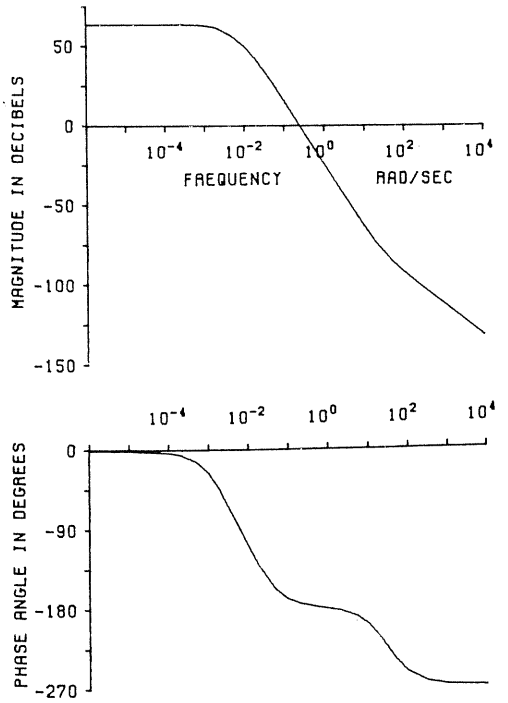

Fig. 5 Frequency response of cell A bed temperature with respect to cell A coal feed rate

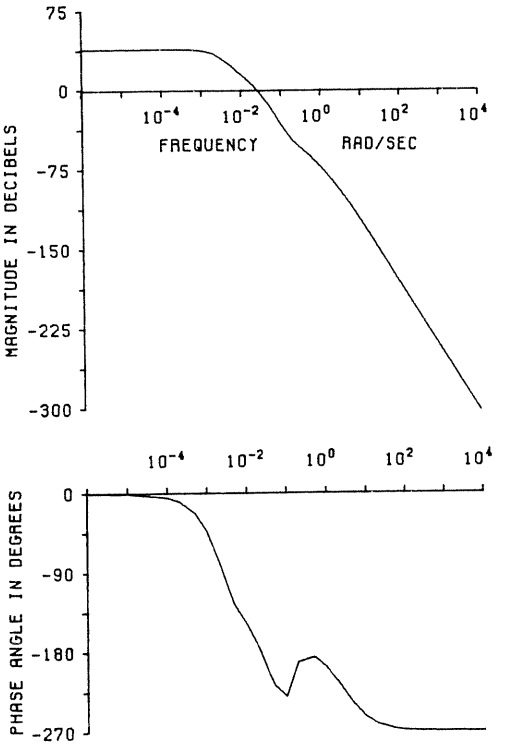

Fig. 6 Frequency response of cell B bed temperature with respect to cell A coal feed rate.

(Fig. 7b), cell B bed temperature increases monotonically to a new steady-state value (1428°F), because a smaller amount of energy is carried away by reduced flue gas flow. This reduces furnace exit pressure which increases cell A air flow slightly (0.32%), causing a small reduction (1°F) in cell A bed temperature. Decreased cell B flue gas flow reduces convective heat transfer in freeboard and convective regions, reducing drum steam pressure. Subsequently, as cell B bed temperature continues to increase, more energy is transferred to submerged waterwall and evaporator tubes, and drum pressure partially recovers. Main steam pressure, temperature, and flow settle at new steady-state values of bit lower than the original values.

A 5% step increase in steam flow control valve area (Fig. 7c) causes a monotonic decrease of steam pressure to a new steady-state value (476 psia) and a small increase (+0.5%) in steady-state steam flow following an initial transient. Since cell A contains immersed superheaters, its bed temperature is lowered slightly because of increased convective heat transfer to steam inside the superheater tubes. Cell B bed temperature is practically unaffected (change less that 1°F) because its immersed evaporator tubes contain boiling water at drum saturation conditions which change very little following the disturbance. Air flows through cells A and B remain undisturbed.

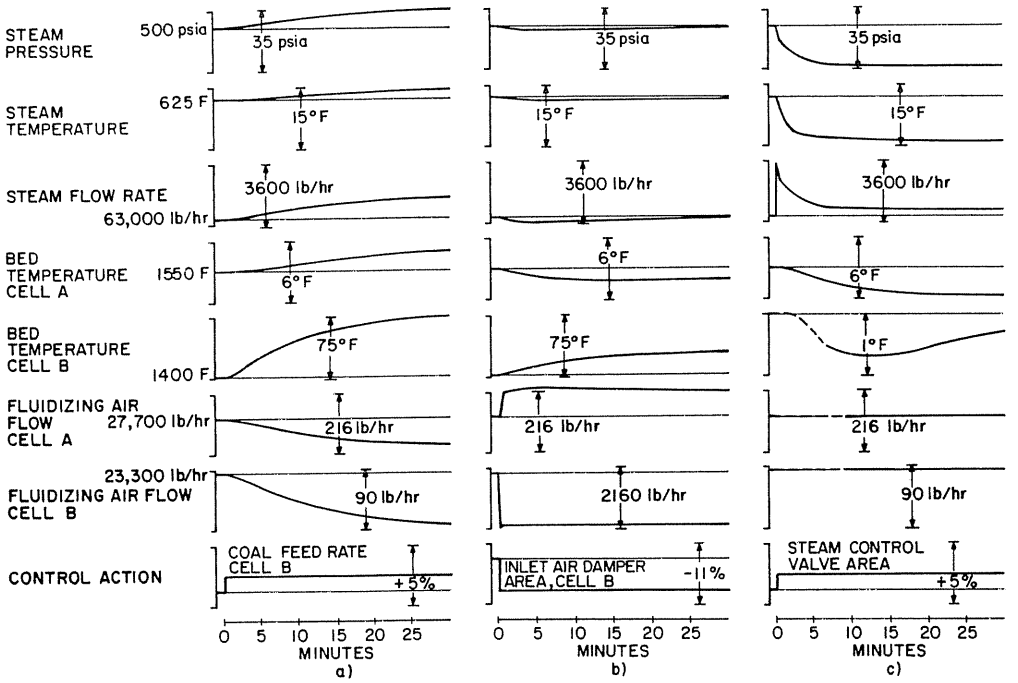

Fig. 7 Transient response following step changes in a) cell B coal feed rate, b) cell B inlet air damper area, and c) steam flow control valve area.

The transient responses just discussed characterize process dynamics and interaction within and among each of the three cells. In steering a multicell fluidized-bed steam generator rapidly and safely from one load to another, a controller is required that accomodates process interactions, particularly in load following duty. Figure 7 shows the strong coupling between heat transfer and combustion processes in the fluidized bed. The independent increase in coal feed rate and decrease in fluidizing air flow both cause an increase in bed temperature; in each case, it is a consequence of the decreased air-to-fuel ratio. However, the independent increase in coal feed rate and decrease in fluidizing air flow tend to change steam temperature and pressure in opposite directions, and with different time responses: a slow rise in steam conditions following coal flow increase; a more rapid decline following air flow decrease with a slight overshoot and subsequent slower recovery as bed temperature readjusts.

The need to control bed temperature, as well as steam pressure, distinguishes the fluidized-bed boiler from a conventional pulverized fuel or oil-fired boiler in which there is no corresponding flame temperature control. Coal feed rate and air flow (damper position) can be used individually in simple control loops to regulate bed temperature and steam pressure, respectively, or vice versa, or can be used jointly to control both process variables in an integrated manner. With coal feed rate and air flow controlled separately, air-to-fuel ratio can no longer be guaranteed, particularly if bed temperature is to be constant independent of load. A load-dependent bed temperature set point can be a consequence of the need to control both bed temperature and steam pressure, while maintaining acceptable air-to-fuel ratio.

Conclusion

A dynamic model of a multicell, atmospheric-pressure, fluidized-bed combustion system has been formulated in state-space form, using a modeling technique verified experimentally for a single-cell fluidized-bed combustion test plant. Numerical results have been obtained by digital simulation of the plant model.

The model can be linearized at several steady-state operating points. Eigenvalue analysis shows that (open-loop) plant response slows down with decreasing load. Transient responses of the nonlinear model demonstrate the interactive characteristics of a multicell fluidized-bed steam generator.

The model presented in this paper provides information for understanding interactive process dynamics, and for designing an interactive multivariable controller. It is the basis from which to predict effects of a subsystem change on the entire process and to study overall system performance.

Appendix: State, Control (Input), and Output Variables

The model has state variables x, control (input) variables u, and output variables y. (The listed y variables are those required for controller design.)

State Variables x

Combustion rates in cells A, B, and C fluidized beds
Average fluidized bed temperatures in cells A, B, and C
Average flue gas temperatures in cells A, B, and C freeboard regions
Average waterwall tube temperatures in cells A, B, and C fluidized beds, freeboard regions, and convection regions
Average primary and secondary superheater tube wall temperatures in cell A
Average immersed evaporator tube wall temperature in cell B
Convection zone evaporator tube wall temperatures in cells A and B
Convection zone economizer tube wall temperature in cell C
Flue gas density and temperature at exhaust duct
Average tube wall temperature in air preheater
Attemperator steam density, and enthalpy
Control valve steam density, and enthalpy
Drum steam density
Drum water volume‡
Mass of fluidized bed solids in cells A, B, and C‡

Control (Input) Variables u

Coal feed rate in cells A and B
Coal plus fly ash feed rate in cell C
Limestone feed rates in cells A, B, and C
Air flow damper areas in cells A, B, and C
Spray water valve area
Main steam valve area
Feedwater valve area (not presently used in the model)

Output Variables y

Average fluidized-bed temperatures in cells A, B, and C
Main steam flow, temperature, and pressure
Flue gas pressure at exhaust duct
Drum water level

Acknowledgments

This work was supported by the Coal Conversion and Utilization Division of the U.S. Energy Research and Development Administration (Department of Energy) under Contract Number EX-76-C01-2453.

References

[1] Berkowitz, D. A., Ray, A., Sumaria, V., and Wilson, M., "Dynamic Modeling, Testing, and Control of Fluidized Bed Systems," *5th International Conference on Fluidized Bed Combustion*, Washington, D. C., Dec. 1977.

[2] Lin, Y., Nielsen, R. S., and Ray, A., "Fuel Controller Design in a Once-Through Subcritical Steam Generator System," *Transactions of the ASME, Journal of Engineering for Power*, Vol. 100, Jan. 1978, pp. 189-196.

[3] Berkowitz, D. A., (ed.) *Proceedings of the Seminar on Boiler Modeling*, The Mitre Corporation, Bedford, Mass., Oct. 1975.

[4] Morgantown Energy Research Center, *Conceptual Design for Fluidized-Bed Combustion/Component Test Integration Unit*, Proposal No. U 60501 CA, Morgantown, W. V., Feb. 1976.

[5] Wilson, J. S. and Gillmore, D. W., "Conceptual Design of Atmospheric Fluid-Bed Component Test and Integration Unit," *Proceedings of the 4th International Conference on Fluidized-Bed Combustion*, Washington, D. C., Dec. 1975, pp. 187-197.

[6] Berkowitz, D. A. and Ray, A., "Fluidized Bed Boiler Dynamics, Control, and Testing," Paper No. 31, *Proceedings of the 3rd Power Plant Dynamics, Control and Testing Symposium*, Knoxville, Tenn., Sept. 1977.

[7] Kunii, D. and Levenspiel, O., *Fluidization Engineering*, Wiley, New York, 1969.

[8] Adams, J., Clark, D. R., Louis, J. R., and Spanbauer, J. P., "Mathematical Modeling of Once-Through Boiler Dynamics," *IEEE Transactions on Power Apparatus and Systems*, Vol. 84, Feb. 1965, pp. 146-156.

[9] Kwatny, H. G., McDonald, J. P., and Spare, J. H., "A Nonlinear Model for Reheat Boiler-Turbine-Generator Systems: Part II – Development," *Proceedings of the Joint Automatic Controls Conference*, St. Louis, Mo., 1971, pp. 227-236.

[10] McNamara, R. W., Ringham, M. R., Bramblett, C. C., and Southworth, L. C., "Practical Simulation of an Industrial Fluid System with Controls – The Circulator Auxiliaries for the Fort St. Vrain Nuclear Generating Station," *Proceedings of the Joint Automatic Controls Conference*, San Francisco, 1977, pp. 345-350.

[11] Ray, A. and Bowman, H. F., "A Nonlinear Dynamic Model of a Once-Through Subcritical Steam Generator," *Transactions of the ASME, Journal of Dynamic Systems, Measurement and Control*, Ser. G, Vol. 98, Sept. 1976, pp. 332-339.

[12] Ray, A., Berkowitz, D. A., and Sumaria, V., "Mathematical Modeling and Digital Simulation of the MERC Component Test and

‡These state variables have been set to constant values in the open-loop model; the corresponding differential equations have been solved algebraically.

Integration Unit," The Mitre Corporation, Bedford, Mass., Rept. No. MTR-3447, May 1977.

[13] Rohsenow, W. M. and Hartnett, J. P., (eds.), *Handbook of Heat Transfer*, McGraw Hill, New York, 1973.

[14] *Steam/Its Generation and Use*, Babcock and Wilcox, New York, 1972.

[15] Holman, J. P., *Heat Transfer*, McGraw Hill, New York, 1976.

[16] Beer, J. M., Baron, R. E., Borghi, G., Hodges, J. L. and Sarofim, A. F., "A Model of Coal Combustion in Fluidized Bed Combustors," *5th International Conference on Fluidized-Bed Combustion*, Washington, D. C., Dec. 1977.

[17] Shames, I. H., *Mechanics of Fluids*, McGraw Hill, New York, 1962.

[18] Ray, A., "Approximation of Fundamental Equations for Finite-Dimensional Modeling of Thermo-Fluid Processes," *Transactions of the ASME, Journal of Engineering for Power*, Vol. 100, Oct. 1978 (to be published).

[19] MacFarlane, A.G.J., "A Survey of Some Recent Results in Linear Multivariable Feedback Theory," *Automatica*, Vol. 8, July 1972, pp. 455-492.